ICAS 2021 SHANG HAI
International Council of the Aeronautical Sciences
32nd Congress of the International Council of the Aeronautical Sciences
September 6-10, 2021
Pudong Shangri-La, Shanghai, China

INVESTIGATION ON DIFFERENT NUMERICAL SIMULATION METHODS OF ROCKET ENGINE

Chen Hao[1], Yang Yifeng[1], Xue Pu[1], Li Xiaoxuan[1], Dong Chao[1], Wang Suozhu[1] & Zhang Mingxing[1]

1 Beijing Institute of Space Long March Vehicle, Beijing 100076, China

Abstract

Different numerical simulation methods of rocket engine based on CFD have been investigated on gas model, inlet boundary condition and computational domain. Based on this investigation, an efficient numerical simulation method of rocket engine with acceptable accuracy has been recommended to the engineers for their reference.

Keywords: numerical simulation, rocket engine, gas model, computational domain

1. Introduction

The small rocket engine based on chemical energy is an effective means for spacecraft attitude control, and the calculation method based on CFD can also achieve accurate thrust evaluation[3~5]. However, for the industry, the evaluation method not only needs to be accurate enough, but also needs to be fast enough to achieve iterative optimization design.

In the CFD based evaluation method, the gas model, boundary condition and computational domain are variables that can be adjusted to make a trade-off between accuracy and computational efficiency. The gas model based on the real components is more accurate than the one component gas model based on the equivalent specific heat ratio, but the computational efficiency is lower due to the additional component equations. In terms of inlet boundary conditions, the stagnation pressure-temperature boundary and the mass-flow-temperature boundary can be converted equivalently, while the computational efficiency and accuracy of the two boundary conditions need to be evaluated. In the computational domain, the integration method considering internal and external flow is more accurate than the method only considering internal flow, but the computational time increases with the increase of the grid number.

In this paper, the CFD method is used to investigate the gas model, inlet boundary condition and computational domain. The deviations introduced by the approximate simplification of the equivalent single component gas model and the internal flow only computational domain are studied. The applicability of the stagnation pressure-temperature boundary and the mass-flow-temperature boundary is researched. On this basis, an efficient numerical simulation method with acceptable accuracy is proposed.

2. Computational Method

In this paper, the finite volume method (FVM) is used to solve the Navier-Stokes equations[1] (including the component transport equations) in the two-dimensional axisymmetric coordinate system, while the chemical reactions and turbulence effects are not considered.

$$\frac{\partial}{\partial t}\int_{\partial\Omega} Q dv + \int_{\partial\Omega} F \cdot \hat{n} dS = \int_{\partial\Omega} G \cdot \hat{n} dS \quad (1)$$

Where: $\mathrm{Q} = [\rho \quad \rho u \quad \rho v \quad \rho E \quad \rho\gamma_i]$, F is the inviscid flux, G is the viscous flux, and the related expressions are listed as follows.

$$F = \begin{bmatrix} \rho V \\ \rho u V + n_x P \\ \rho v V + n_y P \\ \rho H V \\ \rho \gamma_i V \end{bmatrix} \tag{2}$$

$$G = \begin{bmatrix} 0 \\ n_x \tau_{xx} + n_y \tau_{xy} \\ n_x \tau_{yx} + n_y \tau_{yy} \\ n_x(u\tau_{xx} + v\tau_{xy} + q_x) + n_y(u\tau_{yx} + v\tau_{yy} + q_y) + \sum_{j=1}^{n} \rho D_j H_j \left(\nabla \cdot (\nabla \gamma_j)\right) \\ \rho D_i (\nabla \cdot (\nabla \gamma_i)) \end{bmatrix} \tag{3}$$

Where: V is the inverse velocity, u,v,w are the three velocity components, and n_i is the component of the unit vector in the coordinate system; P is pressure, E is total energy, ρ is density, H is total enthalpy; γ_j is the mass fraction of the j-th gas, H_j is the total enthalpy of the j-th gas, D_j is the diffusion coefficient of the j-th gas; τ_{ij} is the stress tensor term, q_i is the heat conduction term.

When the equations are solved, the inviscid flux is calculated by the Ausm+up scheme[2] and the limiter is the minmod scheme. LUSGS scheme is used in time advancing. In terms of boundary conditions, the non-slip boundary is used on the wall surface, the non-reflection condition based on Riemann-invariants is used as a far-field boundary for the internal and external flow integration method, and the pressure imposed boundary is used at the outlet position for the internal flow only method.

3. Cases Description

The nozzle profile of the rocket engine adopted in this paper is shown in Figure 1. The computational grid for the nozzle is shown in Figure 2. There are 5 kinds of boundary condition shown in different colours, such as: external far-field in purple, symmetry axis in white, solid wall in blue, internal inlet in red, and internal exit in yellow.

In order to ensure the computational accuracy, the grid is refined near wall surface and throat. The grid in Figure 2 will be directly used in the internal and external flow integration method, and only the grid inside the nozzle will be retained in the internal flow only method.

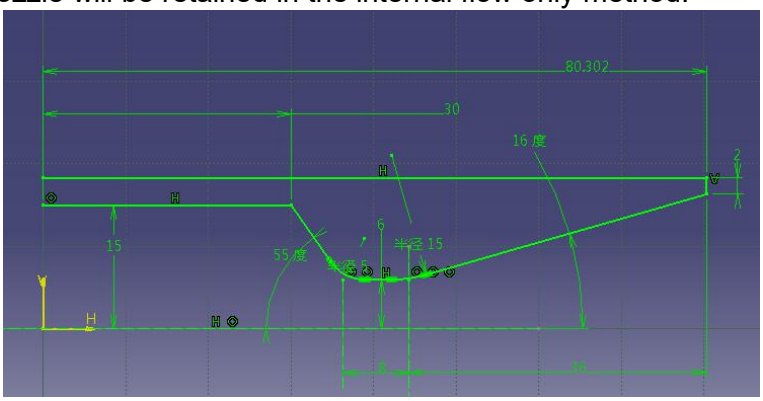

Figure 1 – Nozzle profile of the rocket engine

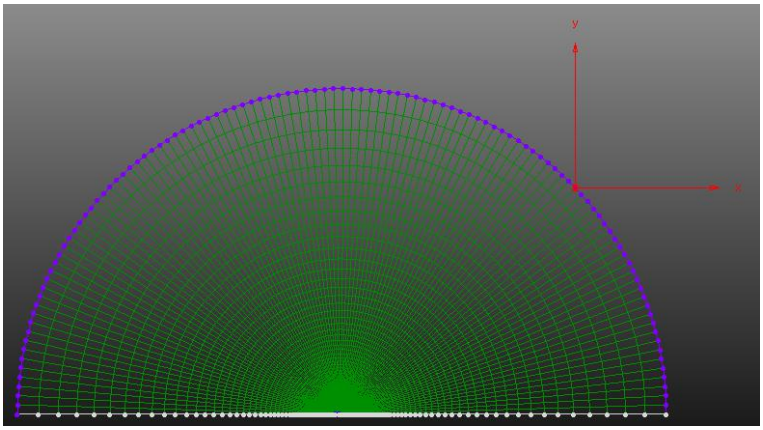

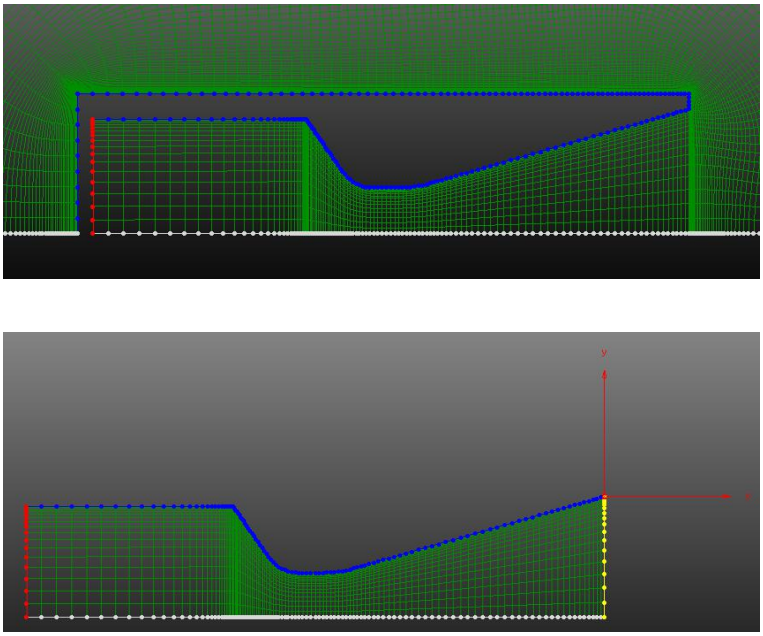

Figure 2 – Computational grid

The components and properties of the internal engine gas are shown in Table 1 which will be used in the computational method based on real component gas model.

Table 1 Engine gas properties

Component	Average Molecular Weight (g/mol)	Mass Fraction
CO2	44	0.15092
CO	28	0.53704
H2O	18	0.12546
N2	28	0.13132
H2	2	0.01456

The properties of equivalent one component gas converted from the real components of the engine gas are shown in Table 2. The gas properties will be used in the computation based on the equivalent one component gas model.

Table 2 Equivalent one component gas properties

Specific Heat Ratio	Average Molecular Weight (g/mol)
1.25	24

The inlet boundary conditions of the engine nozzle are shown in Table 3. The equivalent mass flow rate is calculated as follows.

The mass flow through the nozzle is governed by the factor section under supercritical flow conditions which can be expressed by the equation below.

$$\dot{m} = \frac{\Gamma(k)}{\sqrt{R_c T_c}} p_c A_t \tag{4}$$

Where k is the specific heat ratio, $\Gamma(\mathrm{k})$ is the specific heat ratio function, $\mathrm{p_c}$ is the pressure of combustor, $\mathrm{T_c}$ is the temperature of combustor, $\mathrm{A_t}$ is the throat area and $\mathrm{R_c}$ is the universal gas constant.

Table 3 Inlet boundary conditions

Stagnation Pressure （MPa)	Stagnation Temperature （K)	Equivalent Mass Flow Rate （kg/s)
8	2000	0.7153

The far-field boundary conditions in the internal and external flow integration method are shown in Table 4.

Table 4 Far-field boundary conditions

Altitude （km)	Pressure （Pa)	Temperature （K)
20	5529.31	216.65

The cases computed in this paper are described in Table 5. By comparing case 1 with case 2, 3 and 4, the effects of different gas models, different inlet boundaries and different computational domains on the accuracy and efficiency of the engine jet flow can be obtained.

Table 5 Cases description

Name	Gas Model	Inlet Boundary	Computational Domain
case 1	Real Components	Stagnation Pressure-Temperature	Internal and External Flow
case 2	Equivalent Single Component	Stagnation Pressure-Temperature	Internal and External Flow
case 3	Real Components	Mass-Flow-Temperature	Internal and External Flow
case 4	Real Components	Stagnation Pressure-Temperature	Internal Flow only

4. Results and Discussions

4.1 Real Components Model vs Equivalent One Component Model

The computing time and thrust of the different gas models are compared in Table 6. The results show that by after using the simplified equivalent one component gas model, the thrust deviation is 0.95%, and the computational efficiency is increased by 2.5 times.

Table 6 Comparison of cases with different gas models

Name	Gas Model	Computing Time （s)	Thrust （N)
case 1	Real Components	527	1456.2
case 2	Equivalent One Component	211	1470.0

The Mach number distribution and pressure distribution obtained by different gas models are shown in Figure 3 and Figure 4 respectively. It can be seen that the Mach number distribution and the pressure distribution at the outlet are slightly different after using the simplified equivalent one component gas model.

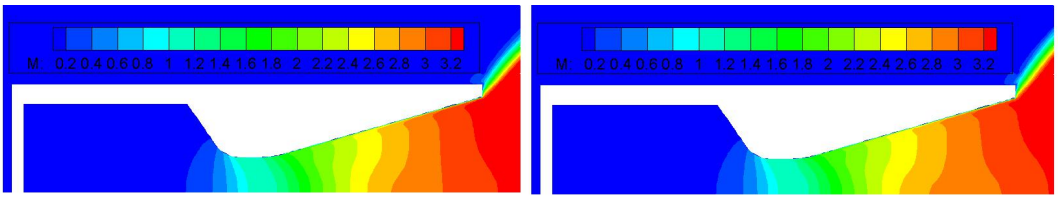

1) case 1 2) case 2

Figure 3 – Mach number distribution of different gas models

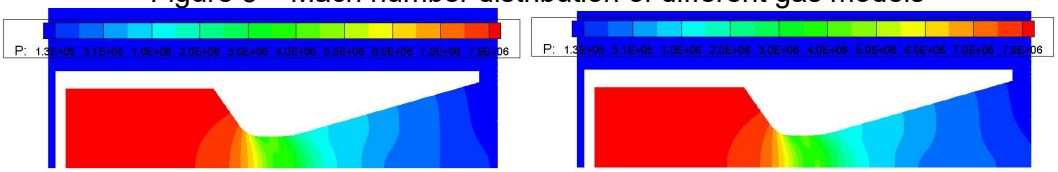

1) case 1 2) case 2

Figure 4 – Pressure distribution of different gas models

4.2 Stagnation Pressure-Temperature Boundary vs Mass-Flow-Temperature Boundary

The computing time and thrust of the different inlet boundaries are compared in Table 7. The results show that using different inlet boundary will only result in 2.0% thrust deviation and 8.7%

computing time variation.

Table 7 Comparison of cases with different inlet boundaries

Name	Inlet Boundary	Computing Time（s)	Thrust（N)
case 1	Stagnation Pressure-Temperature	527	1456.2
case 3	Mass-Flow-Temperature	573	1485.3

The Mach number distribution and pressure distribution obtained by different inlet boundary conditions are shown in Figure 5 and Figure 6 respectively. It can be found that the Mach number distribution and pressure distribution are basically the same.

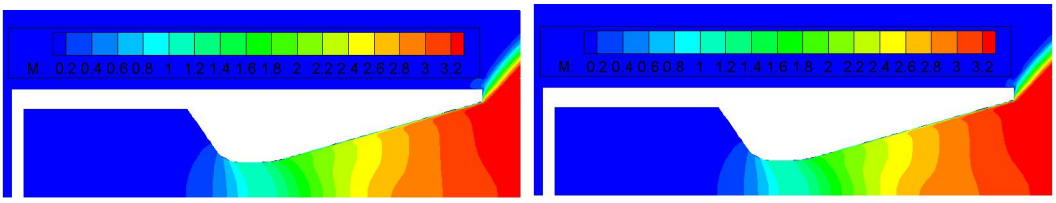

1) case 1　　2) case 3

Figure 5 – Mach number distribution of different inlet boundary conditions

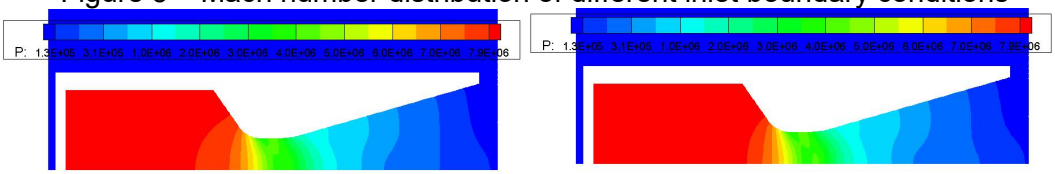

1) case 1　　2) case 3

Figure 6 – Pressure distribution of different inlet boundary conditions

4.3 Internal and External Flow Integration Method vs Internal Flow only Method

The computing time and thrust of the cases with different computational domains are compared in Table 8. The results show that by adopting the simplified method of internal flow only, the thrust deviation is 0.06%, and the computational efficiency is increased by 14.2 times.

Table 8 Comparison of Cases with Different Computational Domains

Name	Computational Domain	Computing Time（s)	Thrust（N)
case 1	Internal and External Flow	527	1456.2
case 4	Internal Flow only	37	1457.1

The Mach number distribution and pressure distribution obtained in different calculation regions are shown in Figure 7 and Figure 8 respectively. It can be seen that the Mach number distribution and the pressure distribution at outlet are slightly different.

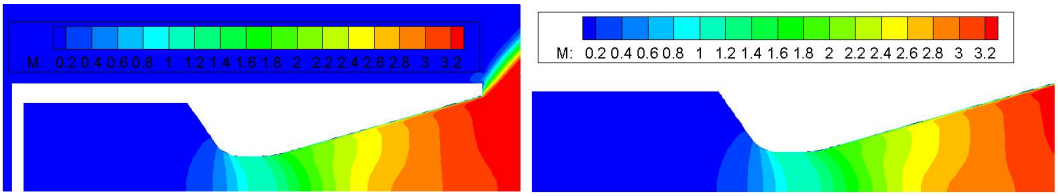

1) case 1　　2) case 4

Figure 7 – Mach number distribution of different computational domains

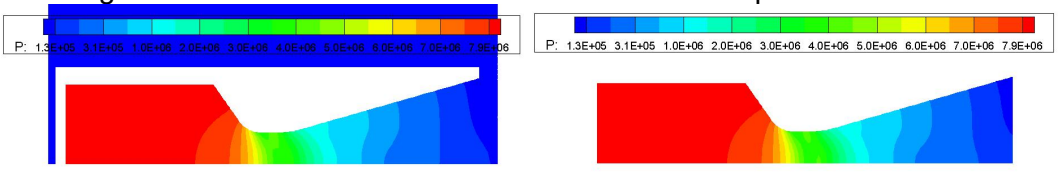

1) case 1　　2) case 4

Figure 8 – Pressure distribution of different computational domains

5. Conclusion

In this paper, CFD method is used to study the deviation of different numerical simulation methods of rocket engine from three aspects of gas model, inlet boundary condition and computational domain. The main conclusion are listed below.

The thrust differs only 0.95% when using the simplified equivalent one component gas model, and the computational efficiency increases by 2.5 times. Therefore, the computational efficiency can be improved by using the simplified gas model without affecting accuracy.

The stagnation pressure-temperature inlet boundary condition and the mass-flow-temperature inlet boundary condition are equivalent both in computational accuracy and efficiency.

The thrust result is nearly affected by adopting the simplified internal flow only method, while the computational efficiency can be increased by 14.2 times. Thus the computational efficiency can be significantly improved without affecting accuracy by computing internal flow only.

Considering the computational accuracy and efficiency, it is suggested that the simplified method by computing internal flow only should be used to evaluate the thrust of rocket engine in engineering design.

6. Contact Author Email Address

To contact us, please mail to: tdchenhao@126.com

7. Copyright Statement

References

[1] Hirschel, E H, and Weiland C. *Selected Aerothermodynamic Design Problems of Hypersonic Flight Vehicles*. Springer Berlin Heidelberg, 2009.

[2] Liou M. A sequel to AUSM, Part II: AUSM + -up for all speeds[J]. *Journal of Computational Physics,* Vol. 214, No. 1, 2006.

[3] Jentink T . CFD code validation for nozzle flowfields[C]. *27th Joint Propulsion Conference*, 1991.

[4] Syed S , Erhart J , King E . Application of CFD to pitch/yaw thrust vectoring spherical convergent flap nozzles[C]. *Joint Propulsion Conference*, 2013.

[5] Bukhari B , Zahir S , Khan M , et al. A Cfd-Experimental Comparison for a Low Thrust Satellite Nozzle with Estimation of Forces on a Jet Vane Placed at Supersonic Exhaust[C]. *Aiaa Aerospace Sciences Meeting & Exhibit*, 2006.